





Article

Sensor-Assisted Assessment of the Tribological Behavioral Patterns of Al–SiC_p Composites under Various Environmental Temperature Conditions

Manivannan S ¹, Senthil Kumaran S ² , Srinivasan Narayanan ² , Kathiravan Srinivasan ³ 
and Alex Noel Joseph Raj ^{4,*} 

¹ Department of Mechanical Engineering, Karpagam Academy of Higher Education, Coimbatore - 641 021, Tamil Nadu, India; manivannan.s@kahedu.edu

² Department of Manufacturing Engineering, School of Mechanical Engineering, Vellore Institute of Technology (VIT), Vellore - 632 014, Tamil Nadu, India; senthilkumaran.s@vit.ac.in (S.K.S.); srinivasan.narayanan@vit.ac.in (S.N.)

³ School of Information Technology and Engineering, Vellore Institute of Technology (VIT), Vellore - 632 014, Tamil Nadu, India; kathiravan.srinivasan@vit.ac.in

⁴ Key Laboratory of Digital Signal and Image Processing of Guangdong Province, Department of Electronic Engineering, College of Engineering, Shantou University, Shantou 515063, Guangdong, China

* Correspondence: jalexnoel@stu.edu.cn; Tel.: +152-1729-0026

Received: 11 November 2019; Accepted: 29 November 2019; Published: 2 December 2019



Abstract: Currently, the use of sensors and supporting technologies has become indispensable in the assessment of tribological behavioral patterns of composites. Furthermore, the current investigation focused on the assessment of the tribological behavior of the Al–SiC_p composite for high-temperature applications. Moreover, the Al–SiC_p composite was fabricated by adapting the liquid metallurgy route with varying weight percentages of SiC_p ($x = 3, 6, \text{ and } 9$). Density, hardness, and high-temperature wear tests were performed to evaluate the hardness and tribological characteristics and properties of modern-day advanced composites. Moreover, the inclusion of SiC_p enhanced the advanced composite materials hardness from 60 HV to 110 HV due to a high degree of refinement of the α -phase. Subsequently, the fabricated samples' wear behavior was assessed by varying the wear parameter viz. the applied load (20 N and 30 N) and sliding distance (250 m, 500 m, 750 m, and 1000 m) with the constant sliding velocity (0.45 m/s) for various temperatures (40 °C, 150 °C, and 250 °C). Moreover, the results revealed that the enhancement in the reinforcement percentage improves the wear resistance. Consequently, the wear rate decreased at 250 °C, possibly owing to the development of the oxide layers. Therefore, the occurrence of delamination and plastic deformation were evidenced in the wear-out surface, thereby depicting the prevalence of delamination and the abrasive wear-mechanism.

Keywords: aluminum; SiC_p; stir casting; high-temperature wear; worn-out surface

1. Introduction

Industry X.0 is pushing manufacturing and production businesses to move forward from conventional practices towards the use of progressive digital technologies to accomplish sustainable development. The emergence and advancement of day-to-day science and technology will augment the necessity for lightweight materials with unique characteristics compared to conventional materials.

Aluminum-based alloys are used for fabricating automobile components like pistons, cylinder heads, cylinder blocks, among others, because of the alloys supreme specific strength and stiffness [1–3]. Furthermore, among the available Al alloys, Al–Si alloys exhibit various unique properties, including large strength-to-weight-rate, excellent castability, less thermal expansion, and high corrosion resistance. Moreover, such alloys exhibit weak wear-resistance that reduces their application in tribological environments (slippage under fretting, loading, degradation of material in sliding condition) [4–7]. This demand has prompted material researchers, product inventors, and manufacturers to explore the area of composite materials. Composite manufacturing was identified as the preeminent method to alter the required properties of the base material by adding suitable reinforcement particles. Amid the available composites, the metal matrix composite (MMC) has a comprehensive range of applications with the potential for use in the aerospace and automobile industries. The MMC is fabricated via various routes that include powder metallurgy, stir casting, squeeze casting, among others. In this work, the stir casting route was considered as the most economical method for the mass production of components [8–12]. These MMC's are reinforced with several organic, carbides, and nitride-based materials that include graphite, graphene, silicon carbide, titanium nitride, among others, to enhance the performance of the base materials [13–16]. In general, these carbide-based ceramic particles are widely deployed as reinforcement agents to enhance the hardness and wear behavior of the Al MMC. In the existing literature, the carbide-based reinforcements are employed as agents to enhance the base material's wear behavior. Moreover, the SiC_p-based hybrid Al MMC was developed by Daniel [17] and his coworker to augment the high temperature wear performance of the Al alloy. Subsequently, the authors studied the wear parameters' performance, including load velocity, sliding-distance, SiC_p particle size, and temperature of the developed MMC. They found that increases in temperature decreased the wear resistance of the MMC. However, decreases in particle size and applied load showed an incremental trend in wear resistance. It was also found that the weight percentage of SiC_p acted as a significant parameter in governing the wear behavior of MMC.

Smrutiranjana et al. [18] devised a stir casting scheme for fabricating an Al–SiC_p composite with a constant wt.% of SiC_p (7.5 wt.%). Moreover, they investigated the wear behavior of the composite with variations in environmental conditions that included dry, alkaline, and aqueous medium with varying wear parameters of applied load and speed. They observed that the wear rate increased with the increment in wear parameters under different environmental conditions and they concluded that the wear rate was maximum for the samples analyzed under an alkaline medium. Khan et al. [19] developed a SiC_p reinforced Al MMC by adopting a stir casting scheme for assessing the wear characteristics of the developed MMC. Consequently, they observed that there was an increase in hardness and wear performance. However, the addition of SiC_p showcased a declining trend in tensile and fatigue strength. They also revealed that the wear rate was minimal for Al MMC under saline and acidic mediums. Rouhi et al. [20] performed a comparative study to assess the wear characteristics of the hybrid-based MMC (SiC_p and MoS₂). Additionally, the experimental outcomes demonstrated that the inclusion of SiC_p up to 10 vol.% and MoS₂ up to 2 vol.% exhibited better wear resistance, thereby leading to a lower wear-rate.

Based on the exhaustive literature survey, it is evident that the inclusion of SiC_p augments the base materials wear performance. However, there are only a few works on the wear behavior of composites under elevated temperatures. In this research, the Al MMC materials dry sliding wear characteristics were explored under distinct temperature ranges. There is a current need to explore the wear behavior of Al MMC under various environmental temperatures to develop a more comprehensive range of applications. Based on the facts above, the present work dealt with the fabrication of Al MMC under varying wt.% SiC_p (0, 3, 6, and 9) and carried out a detail investigation of the wear behavior of developed composites under different environmental conditions.

2. Materials and Methods

Hyper eutectic Al–Si alloy with 13.2% Si was melted in a graphite crucible in an electric resistance furnace and held at 850 °C for an hour to attain a homogeneous composition. After degassing with 1.0 wt.% solid hexachloroethane to remove porosity, the melt was stirred for 5 min at frequent intervals for an hour after adding preheated SiC_p ceramic particles. Then the melt was poured into a cast-iron mold preheated at 300 °C. The cast samples were 160 mm long and 26 mm wide, and the percentage of SiC_p varied from 2.0 to 6.0 wt.% is shown in Figure 1. The Al–SiC_p composite specimens were cut into small pieces (10 mm × 100 mm) for metallography studies. The Keller’s reagent (2.5% HNO₃, 1.5% HCl, 1% HF and 95% H₂O) etchant was used in this study. The experimental composite specimens used in the present work were analyzed for composition using an optical emission spectrometer (OES) (Model ARL 3460 from Thermo Electron Corporation, Switzerland). Table 1 also shows the compositions of the Al–SiC_p composites that were studied in the current research. The microstructural analysis was characterized using the DIC Leica optical microscopy (Model No: DM750M) and scanning electron microscopy (Hitachi SEM, NIT Trichy, Tamil Nadu, India). The current study added different levels of SiC_p to the Al–Si alloy to understand the grain refining efficiency.



Figure 1. Illustrating the cast samples of the developed metal matrix composite (MMC).

Table 1. Chemical Analysis of Base Sample.

Elements	Si	Fe	Cu	Mn	Ni	Zn	Ti	Pb	Ca	Sn
Wt.%	13.2	0.72	1.06	0.219	0.0384	0.59	0.0419	0.079	0.0065	0.038

In the current study, different levels of SiC_p could successfully suppress the formation of coarse dendritic α -Al grains into fine equiaxed grains. The grain refining efficiency of different levels of SiC_p like $x = 3.0, 6.0,$ and 9.0 wt.% was influenced by the formations of heterogeneous nucleation in the melt. The composite contained the fine SiC_p particles during grain refinement with the Al–Si alloy; only SiC_p particles acted as heterogeneous nucleating sites for the Al.

Figure 2 shows the precise control of temperature and load prediction during the wear tests performed by utilizing the pin on a disc machine, where step 1 is influenced by the pin and disc arrangement position for real brake pad application in any automobile. While testing the MMC sample, the pin is stationary when the disc is rotated during contact. The pin is moved in a downward direction towards the direction of rotation of the disc position in the step 2 position. When the contact of the pin moves toward the disc, an enormous amount of heat is produced due to friction. The pin creates a track diameter on the disc upon contact of the two mating parts, and it drives higher heat dissipation during

the respective period. The load is also changed when the pin acts on the disc while testing the sample. The corresponding sensor is mounted on the bottom of the pin and disc location, and simultaneously the heat and load are continuously monitored using a temperature and load sensor. The predicted value of the temperature and load is recorded and then processed by the CPU, followed by presentation using the LabView software.

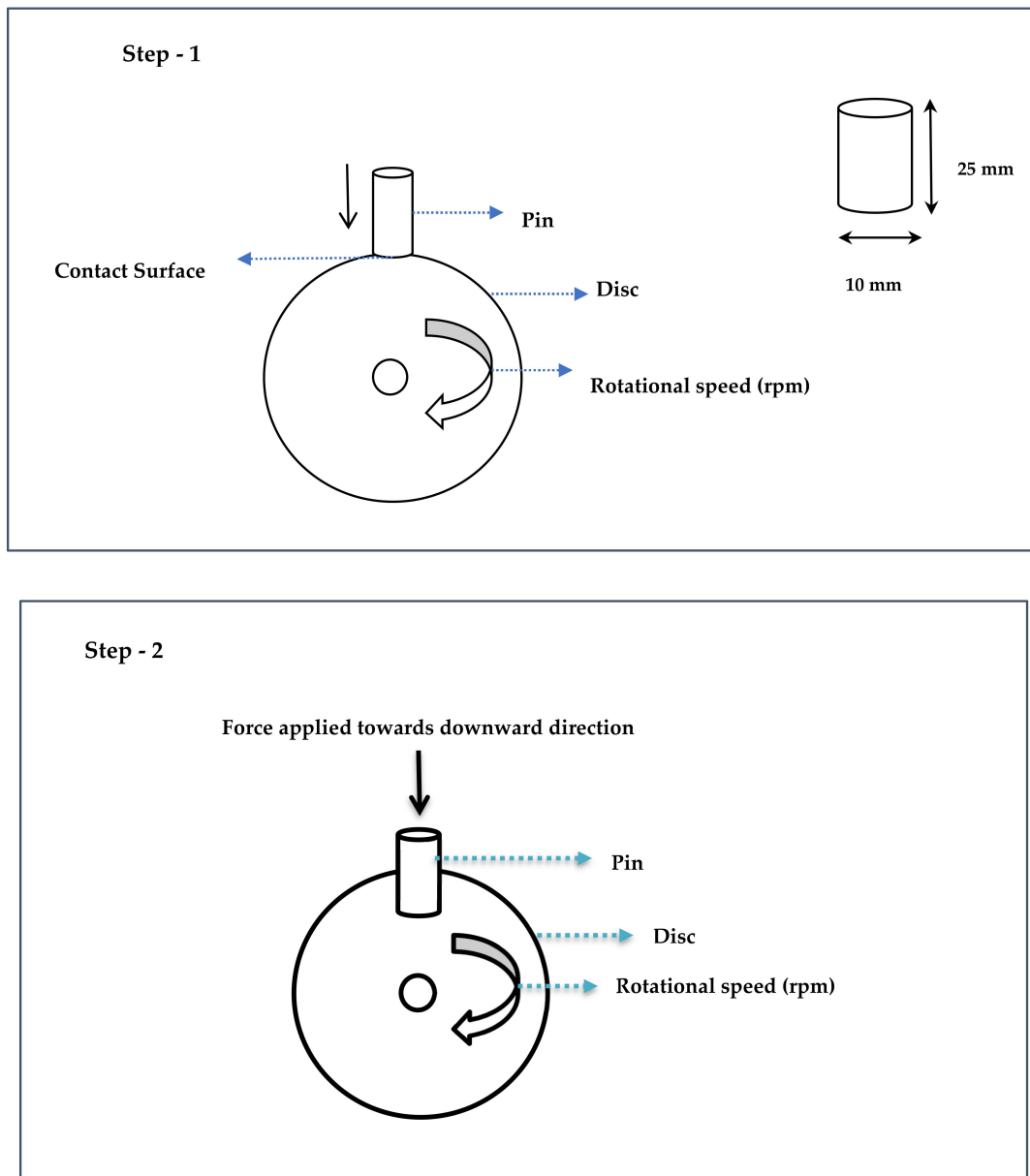


Figure 2. Cont.

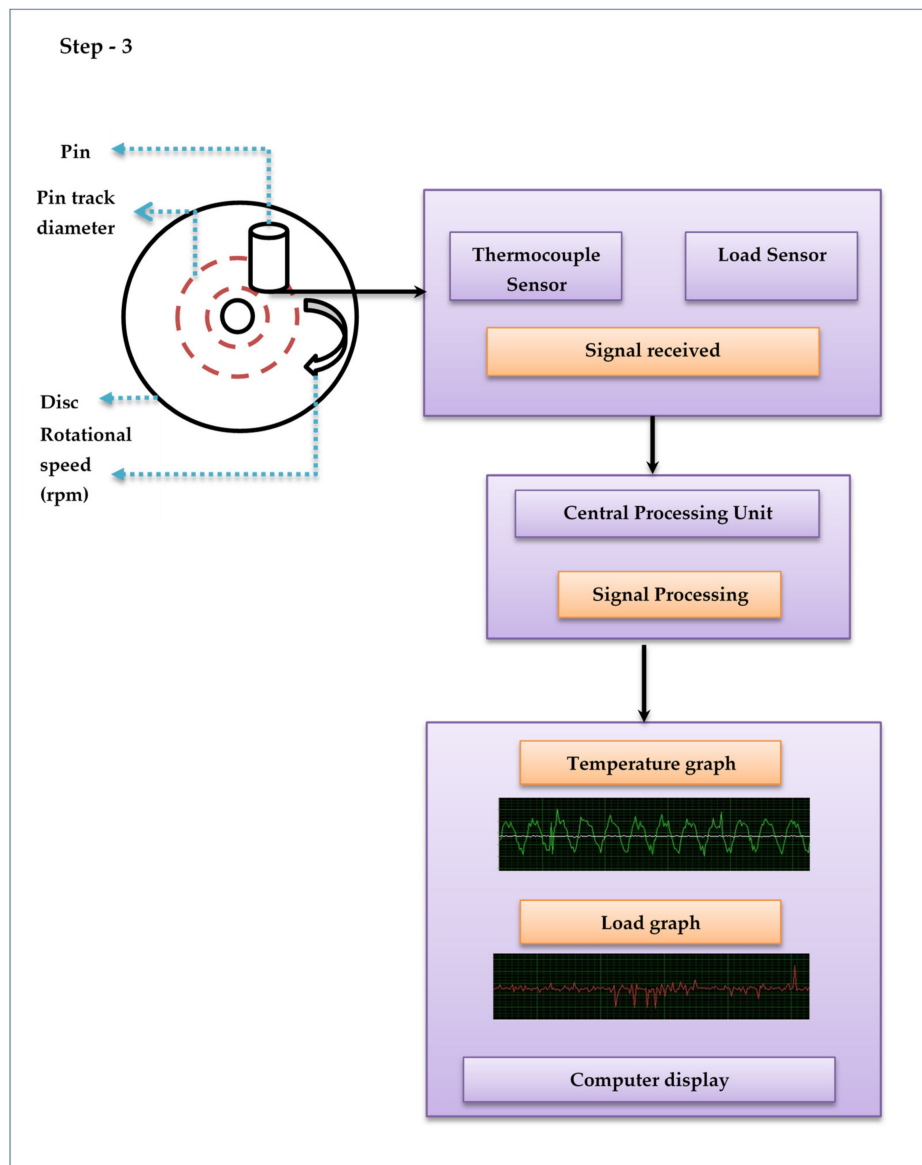


Figure 2. Step 1–3 for temperature and load prediction using different sensors in the tribology test.

3. Material Characterization

The microhardness tests of the fabricated samples were performed using Vickers microhardness testing machine. The applied load during the test was 0.3 kg, with a dwell time of 15 s. The Vickers hardness number (VHN) was calculated from Equation (1).

$$\text{VHN} = (1.854 P)/D^2 \quad (1)$$

where P = applied load, kgf, D = average length of diagonals, mm.

The density tests were conducted using a sartorius electronic balance. High-temperature wear tests were performed on the casted sample pin on the disc apparatus that consisted of the loading panel and controller. The rotating disc was fabricated with carbon steel of diameter 80 mm and hardness of 200 HV. The samples were held stationary, and the required normal load was applied using a lever mechanism. The test was conducted at three different temperatures 40 °C, 150 °C, and 250 °C under two different loading conditions, i.e., 20 N and 30 N, at a fixed sliding velocity of 0.45 m/s. Wear loss of the specimen was measured at four different sliding distances, i.e., 250 m, 500 m, 750 m, and 1000 m.

The pin height was kept at 25 mm, and the diameter was fixed at 8 mm. Wear rate was assessed by measuring the mass loss in the specimen after each wear test and the mass loss, Δm , in the specimen was measured using an electronic weighing machine having a least count of 0.1 mg. Wear rate, which relates to the mass loss (Δm) and sliding distance (L), was calculated using Equation (2),

$$W = \Delta m/L \quad (2)$$

4. Result and Discussion

To understand the mechanism of grain refinement of Al/SiC_p composites, the Al-13.2% Si alloy was modified with various levels of SiC_p like 2.0 wt.%, 4.0 wt.%, and 6.0 wt.% and the melt was poured into a water-cooled water mold of 32 K/s cooling at 5 min holding. The higher cooling rate was chosen to observe the SiC_p particles since a higher cooling rate allows the complete formation of SiC_p fine particles in the Al/SiC_p composites. The samples were subjected to DIC Leica optical microscopy (Figure 3) and SEM microanalysis (Figure 4) to observe the reaction of SiC_p with the nucleation particles, which improves wear resistance under various environmental conditions.

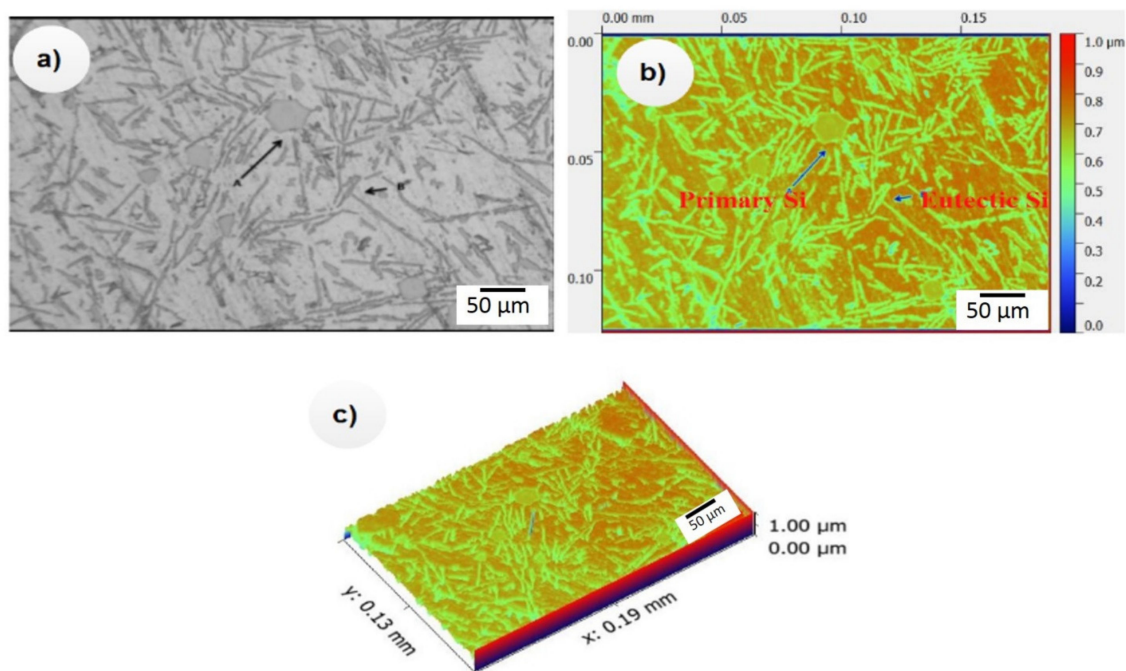


Figure 3. (a–c) Microstructure of the developed Al–Si alloys.

4.1. Microstructural Characterization

Figure 3a–c shows the microstructure of the developed Al–Si alloys. It could clearly show that the Al–Si alloy microstructure consisted of the eutectic mixture and primary Si. Figure 4a–c shows the microstructure of Al-13 wt.% of Si to which 2.0 wt.% SiC_p, 4.0 wt.% SiC_p and 6.0 wt.% SiC_p, respectively, was added. The microstructure analysis also confirmed that the addition of SiC_p refined the eutectic mixture from a coarser to a fine fibrous structure. However, we observed several unidentified needles, formed either by the cleaning of the extracted particle or from Al₄C₃ possibly formed along with the SiC_p particles that reacted with the Al matrix. Generally, the Al₄C₃ was not easily identified, and Al₄C₃ is not easy to extract using any conventional procedure. In this study, we overcame the problem by developing a reclamation process that separated all the solid constituents such as reinforcement, reaction product, and insoluble metallic and non-metallic impurities in the composites melt. Using this technique, Al₄C₃ could be extracted even if it was formed in a small amount. However, the pits and porosities were not reflected in the density values because the density experiments were

conducted in the unpolished samples. Moreover, the hardness results reflected only the surface and subsurface properties.

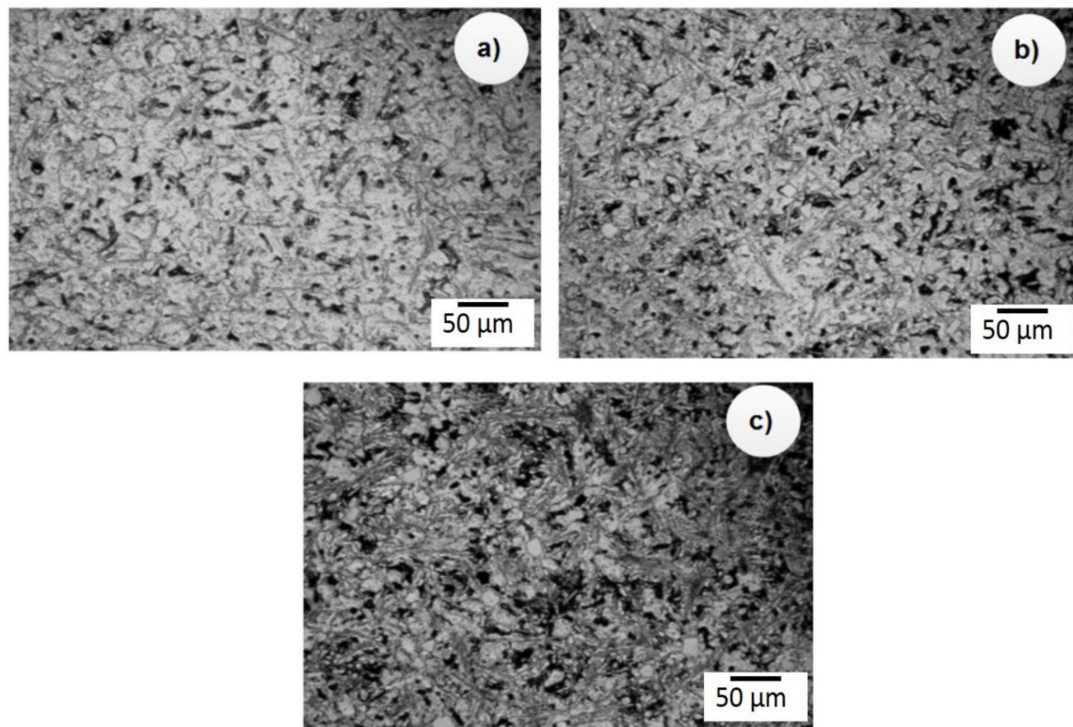


Figure 4. Microstructure of (a) Al-13%Si-2%SiC_p (b) Al-13%Si-4%SiC_p (c) Al-13%Si-6%SiC_p.

4.2. Density Analysis of the Developed Al MMC

The experimental results from the density analysis are shown in Figure 5 showing a slight increment in aluminum density with every addition of SiC_p reinforcement. This increase in aluminum density was due to a higher density of the reinforced silicon carbide (3.21 g/cc). It could be noted from the plot that the density of unreinforced aluminum was near to 2.7 g/cc, which was similar to the actual density of the material that indicated poreless casting.

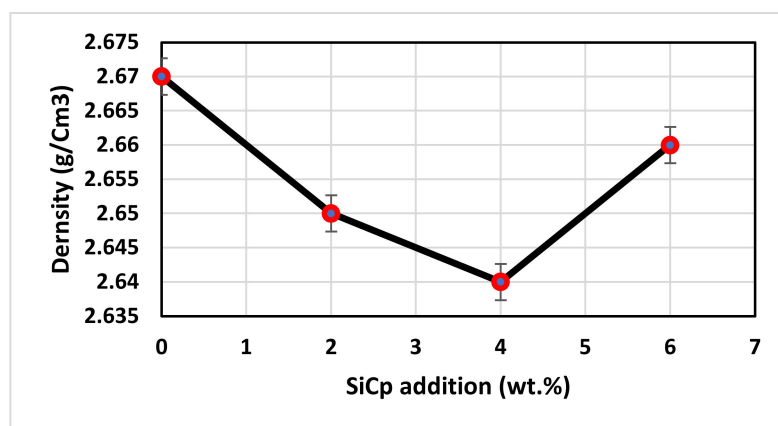


Figure 5. Influence of SiC_p on the Al-Si alloy density.

4.3. Hardness Analysis of the Developed Al MMC

Microhardness results of the unreinforced base alloy and SiC_p reinforced composites are illustrated in Figure 6. The microhardness results indicated a positive trend from the addition of silicon carbide to

the Al alloy resulting in increased hardness from 60 HV to 110 HV for 6% SiC_p addition, which was about 57%. This increment in hardness was due to hindrance offered by the reinforced SiC_p for dislocation motion during plastic deformation when the load was applied. This hindrance to dislocation motion under loading conditions results in an increased load requirement for plastic deformation that indicates the hardness increment [21,22].

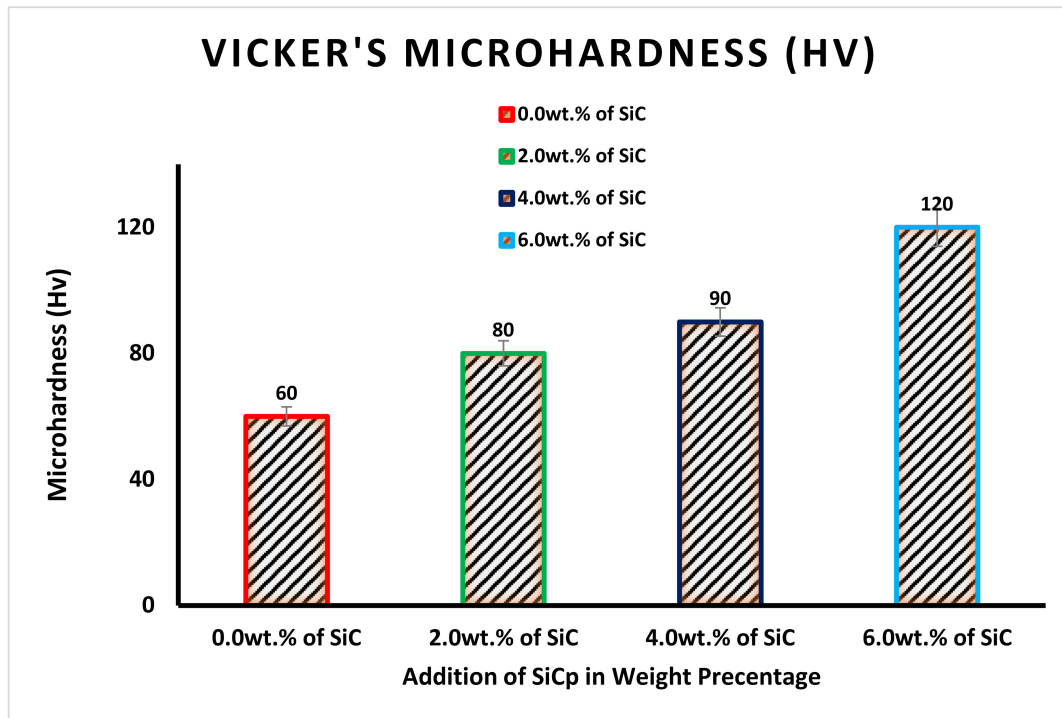
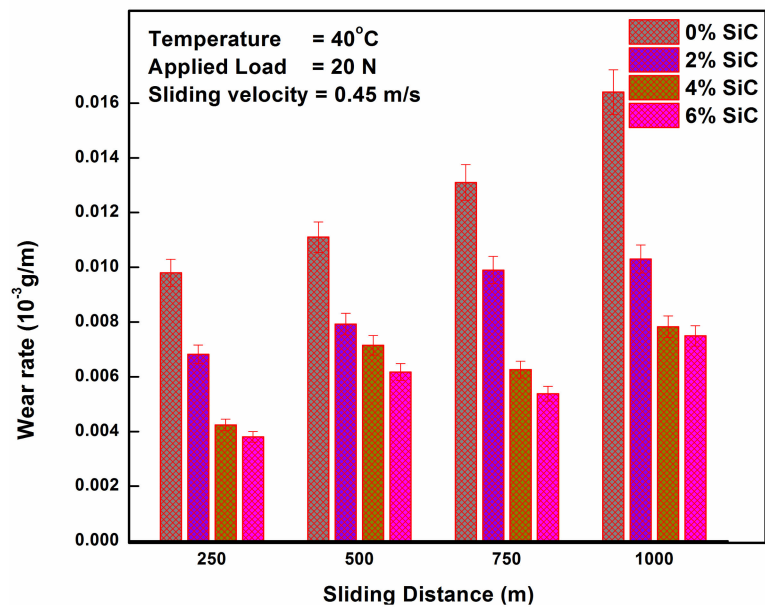


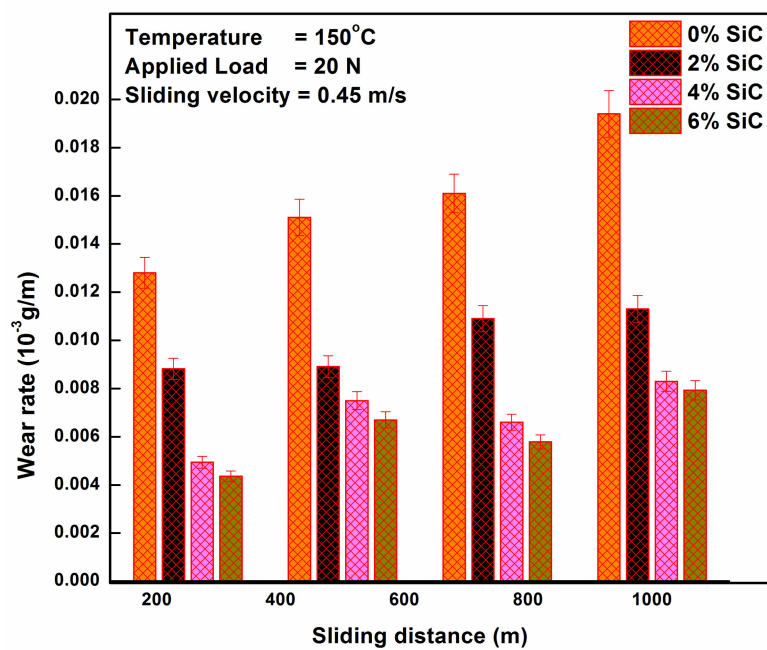
Figure 6. Influence of SiC_p on Al–Si alloy microhardness.

4.4. Wear Behavior of a Developed, Fabricated Composite at Adverse Loading Conditions:

Wear rate observed while testing the aluminum alloy with different SiC_p percentages for different sliding distances is given in Figure 7a. The temperature, load, and velocity were kept constant at 40 °C, 20 N, and 0.45 m/s, respectively. Figure 7b,c depict the wear rate for the same working conditions except for temperature, which was 150 °C and 250 °C, respectively. It is evident from Figure 7a–c that the inclusion of hard SiC_p reinforcement into the soft aluminum matrix results in a decreased wear rate. That is, the wear-resistance capability of the aluminum increases with every addition of SiC_p irrespective of the temperature at which the test is conducted. Moreover, this may be because the hardness of the aluminum increases with SiC_p addition and it is a natural result that harder materials give higher resistance to wear. Since the load required for plastic deformation is higher for harder materials and hence the resistance to wear is also high. The wear rate increases with every increase in sliding distance, as a result of the increased temperature due to increased contact time with the counterpart [8,21,23].

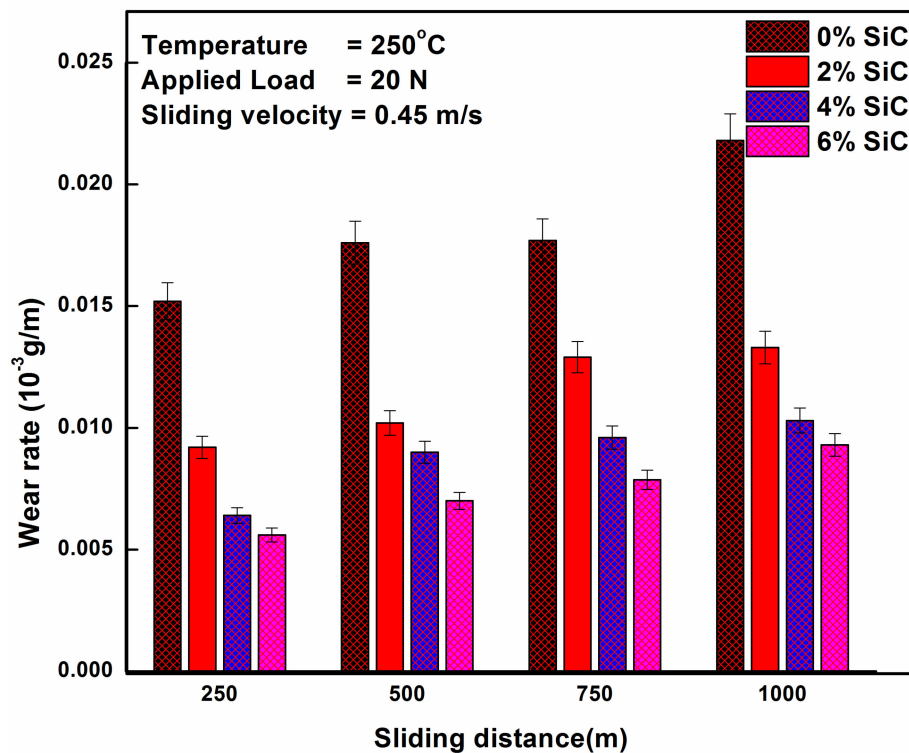


(a)



(b)

Figure 7. Cont.



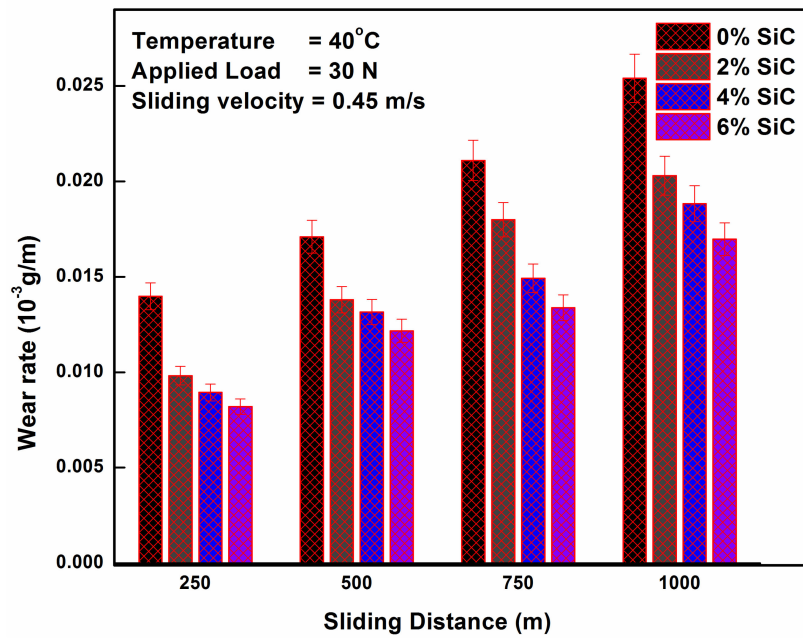
(c)

Figure 7. (a) Wear behavior of the Al MMC at 40 °C under a 20 N load, (b). Wear behavior of the Al MMC at 150 °C under a 20 N load, (c). Wear behavior of the Al MMC at 250 °C under a 20 N load.

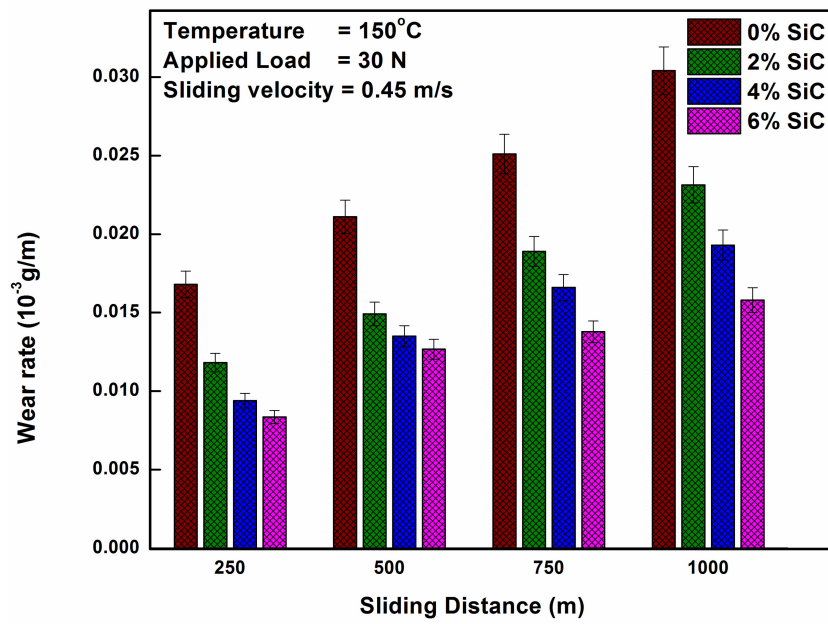
This increased temperature softens the material resulting in more natural plastic deformation and, therefore, higher wear. Furthermore, the increase in the wear rate with sliding distance for unreinforced aluminum is higher than that of reinforced composites, which shows the capability of the developed MMC to withstand severe conditions [24].

While comparing Figure 7a–c, it is evident that the wear rate tends to increase with an increase in the temperature from room temperature (40 °C) to 250 °C. This outcome is because the increase in temperature softens the aluminum and reinforced composites, resulting in higher plastic deformation while sliding. Nevertheless, the increase in temperature causes a proportional increase in the wear rate [23,25].

Figure 8a–c shows the wear rate of the base and reinforced aluminum under different loading conditions while the load applied is 30 N. Comparing Figures 7 and 8, we observed that the rate of wear while sliding increases with an increase in the load from 20 N to 30 N. This increased wear rate at higher loading conditions was due to the increased contact load and the friction between the two sliding parts that tends to increase heat generation at the interface. Moreover, this generated heat results in the softening of the material and higher wear [26–32].

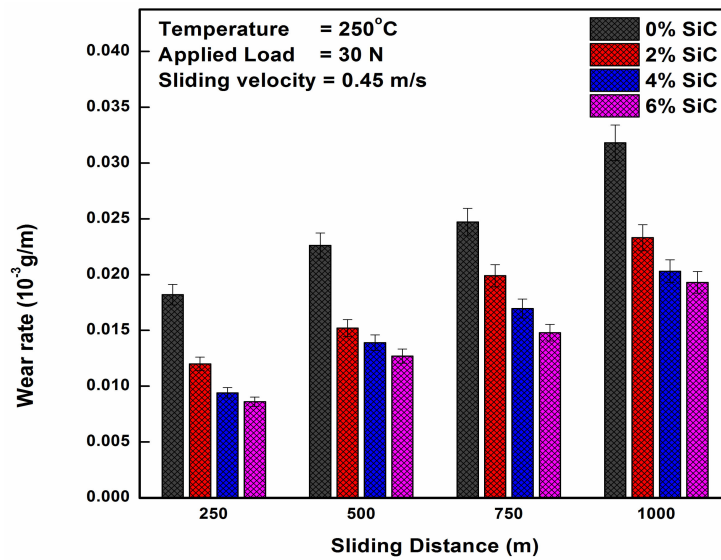


(a)



(b)

Figure 8. Cont.



(c)

Figure 8. (a) Wear behavior of the Al MMC at 40 °C under a 30 N load, (b). Wear behavior of the Al MMC at 150 °C under a 30 N load, (c). Wear behavior of the Al MMC at 250 °C under a 30 N load.

4.5. Worn Out Surface Morphology

Figure 9a–c shows the worn-out surface of the tested Al–Si alloy under varied applied loads of 0 N, 20 N (6 wt.% SiC_p), and 30 N (6 wt.% SiC_p), respectively. The analysis confirmed the occurrence of abrasion and delamination wear over the worn-out surfaces on the pure Al–Si alloy. The Al–13Si alloy with 6 wt.% SiC_p under the 20 N and 30 N applied loads experienced the less abrasion, less debris, and delamination wear.

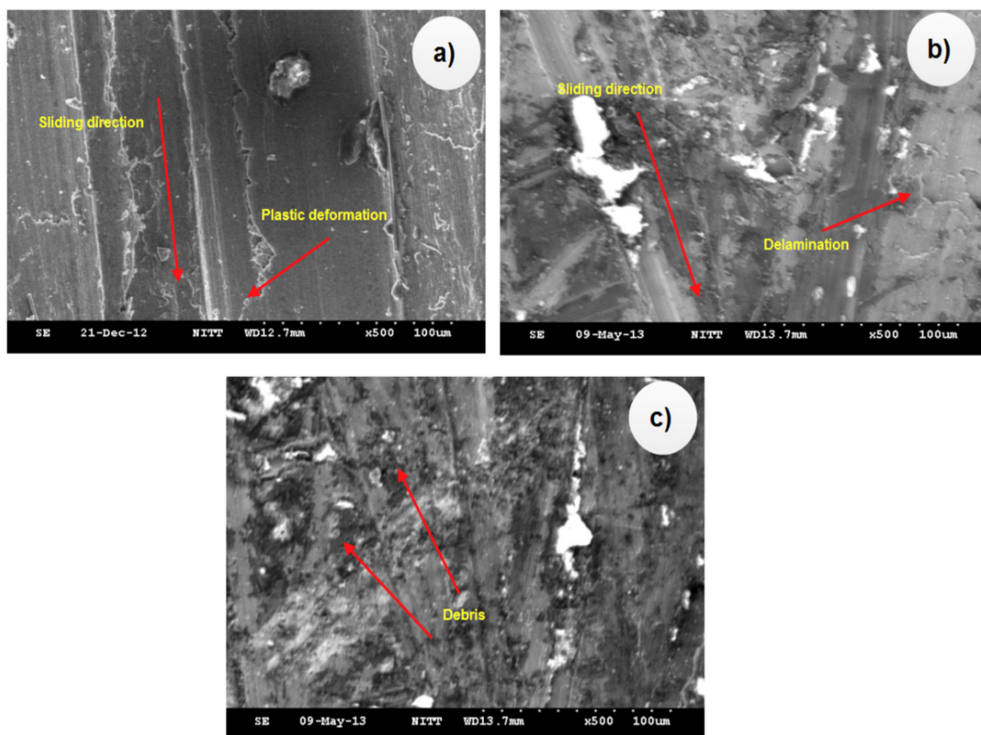


Figure 9. (a) The worn-out surface of the Al–Si matrix, (b) 6 wt.% SiC_p at an applied load of 20 N, (c) 6 wt.% SiC_p at an applied load of 30 N.

5. Conclusions

SiC_p reinforced Al MMC was successfully fabricated through a liquid metallurgy route. The influence of SiC_p over the functional properties of the composite was studied. We investigated the worn-out surface morphology of the samples under wear conditions. The following observations were made:

- The addition of SiC_p resulted in a drastic enhancement in hardness (~57%).
- Increments in SiC_p wt.% showed increments in wear resistance.
- The occurrence of abrasion and delamination wear was observed on the worn-out surface.
- The developed MMC can be practically used in high-temperature sliding applications where higher wear resistance is required. Advanced technologies for tribology behavioral pattern analysis shall be considered in future works [33–36].

The technical merit of this work is summarized as follows:

- (a) The volumetric wear rate decreases with an increasing wt.% of SiC_p, as well as a corresponding decrease in temperature.
- (b) The wear resistance decreases at a higher temperature while it drastically increases with an increase in the wt.% of SiC_p.
- (c) The wear mechanism under the tested conditions was consistently adhesive in nature. The developed composite with a high wt.% of reinforcement agents exhibited abrasive wear mechanisms.

Author Contributions: Conceptualization, M.S. and S.K.S.; methodology, M.S., S.K.S.; software, K.S.; validation, M.S., S.K.S. and S.N.; formal analysis, S.N.; investigation, M.S., S.K.S., S.N.; resources, M.S. and S.K.S.; data curation, K.S.; writing—original draft preparation, M.S. and S.K.S.; writing—review and editing, K.S., S.N. and A.N.J.R.; visualization, S.N. and A.N.J.R.; supervision, A.N.J.R.; project administration, A.N.J.R.; funding acquisition, A.N.J.R.

Funding: This research was funded by the Research Start-up Fund Subsidized Project of Shantou University, China (No. NTF17016).

Conflicts of Interest: The authors declare no conflict of interest.

References

1. Prakash, K.S.; Moorthy, R.S.; Gopal, P.M.; Kavimani, V. Effect of Reinforcement, Compact Pressure and Hard Ceramic Coating on Aluminium Rock Dust Composite Performance. *Int. J. Refract. Met. Hard Mater.* **2016**, *54*, 223–229. [[CrossRef](#)]
2. Kumarasamy, S.P.; Vijayananth, K.; Thankachan, T.; Muthukutti, G.P. Investigations on mechanical and machinability behavior of aluminum/flyash cenosphere/Gr hybrid composites processed through compocasting. *J. Appl. Res. Technol.* **2017**, *15*, 430–441. [[CrossRef](#)]
3. Prakash, K.S.; Gopal, P.M.; Kavimani, V. Effect of rock dust, cenosphere and E-waste glass addition on mechanical, wear and machinability behaviour of Al 6061 hybrid composites. *Indian J. Eng. Mater. Sci.* **2017**, *24*, 270–282.
4. Mahmoud, E.R.I.; Takahashi, M.; Shibayanagi, T.; Ikeuchi, K. Wear characteristics of surface-hybrid-MMCs layer fabricated on aluminum plate by friction stir processing. *Wear* **2010**, *268*, 1111–1121. [[CrossRef](#)]
5. Afkham, Y.; Khosroshahi, R.A.; Rahimpour, S.; Aavani, C.; Brabazon, D.; Mousavian, R.T. Enhanced mechanical properties of in situ aluminium matrix composites reinforced by alumina nanoparticles. *Arch. Civ. Mech. Eng.* **2018**, *18*, 215–226. [[CrossRef](#)]
6. Xu, J.; Qiu, R.; Lian, Z.; Yu, Z.; Yu, P.; Ren, W.; Yu, H. Wear and corrosion resistance of electroforming layer after WEDM for 7075 aluminum alloy. *Mater. Res. Express.* **2018**, *5*, 66502. [[CrossRef](#)]
7. Kumar, S.S.; Uthayakumar, M.; Kumaran, S.T.; Varol, T.; Canakci, A. Investigating the surface integrity of aluminium based composites machined by EDM. *Def. Technol.* **2018**, *15*, 338–343. [[CrossRef](#)]
8. Prakash, K.S.; Kanagaraj, A.; Gopal, P.M. Dry sliding wear characterization of Al 6061/rock dust composite. *Trans. Nonferrous Met. Soc. China* **2015**, *25*, 3893–3903. [[CrossRef](#)]

9. Kavimani, V.; Prakash, K.S.; Pandian, M.A. Influence of r-GO addition on enhancement of corrosion and wear behavior of AZ31 MMC. *Appl. Phys. A Mater. Sci. Process.* **2017**, *123*. [[CrossRef](#)]
10. Prakash, K.S.; Gopal, P.M.; Anburose, D.; Kavimani, V. Mechanical, corrosion and wear characteristics of powder metallurgy processed Ti-6Al-4V/B4C metal matrix composites. *Ain Shams Eng. J.* **2016**. [[CrossRef](#)]
11. Kavimani, V.; Prakash, K.S.; Thankachan, T. Investigation of graphene-reinforced magnesium metal matrix composites processed through a solvent-based powder metallurgy route. *Bull. Mater. Sci.* **2019**, *42*, 39. [[CrossRef](#)]
12. Kavimani, V.; Prakash, K.S. Tribological behaviour predictions of r-GO reinforced Mg composite using ANN coupled Taguchi approach. *J. Phys. Chem. Solids.* **2017**, *110*, 409–419. [[CrossRef](#)]
13. Gopal, P.M.; Prakash, K.S.; Nagaraja, S.; Aravinth, N.K. Effect of weight fraction and particle size of CRT glass on the tribological behaviour of Mg-CRT-BN hybrid composites. *Tribol. Int.* **2017**, *116*, 338–350. [[CrossRef](#)]
14. Kavimani, V.; Prakash, K.S.; Rajesh, R.; Rammasamy, D.; Selvaraj, N.B.; Yang, T.; Prabakaran, B.; Jothi, S. Electrodeposition of r-GO/SiCp nano-composites on Magnesium and its Corrosion Behavior in Aqueous Electrolyte. *Appl. Surf. Sci.* **2016**. [[CrossRef](#)]
15. Kavimani, V.; Prakash, K.S.; Gunashri, R.; Sathish, P. Progress in Organic Coatings Corrosion protection behaviour of r-GO/TiO₂ hybrid composite coating on Magnesium substrate in 3.5 wt.% NaCl. *Prog. Org. Coat.* **2018**, *125*, 358–364. [[CrossRef](#)]
16. Kavimani, V.; Prakash, K.S.; Thankachan, T. Experimental investigations on wear and friction behaviour of SiCp@ r-GO reinforced Mg matrix composites produced through solvent-based powder metallurgy. *Compos. Part B Eng.* **2019**, *162*, 508–521. [[CrossRef](#)]
17. Daniel, S.A.A.; Sakthivel, M.; Gopal, P.M.; Sudhagar, S. Study on tribological behaviour of Al/SiCp/MoS₂ hybrid metal matrix composites in high temperature environmental condition. *Silicon* **2018**, *10*, 2129–2139. [[CrossRef](#)]
18. Pradhan, S.; Ghosh, S.; Barman, T.K.; Sahoo, P. Tribological behavior of Al-SiCp metal matrix composite under dry, aqueous and alkaline medium. *Silicon* **2017**, *9*, 923–931. [[CrossRef](#)]
19. Khan, M.M.; Dixit, G. Evaluation of Microstructure, Mechanical, Thermal and Erosive Wear Behavior of Aluminum-Based Composites. *Silicon* **2019**, 1–12. [[CrossRef](#)]
20. Rouhi, M.; Moazami-Goudarzi, M.; Ardestani, M. Comparison of effect of SiCp and MoS₂ on wear behavior of Al matrix composites. *Trans. Nonferrous Met. Soc. China* **2019**, *29*, 1169–1183. [[CrossRef](#)]
21. Kumar, N.M.; Kumaran, S.S.; Kumaraswamidhas, L.A. An investigation of mechanical properties and corrosion resistance of Al2618 alloy reinforced with Si₃N₄, AlN and ZrB₂ composites. *J. Alloy. Compd.* **2015**, *652*, 244–249. [[CrossRef](#)]
22. Kavimani, V.; Prakash, K.S.; Thankachan, T. Surface characterization and specific wear rate prediction of r-GO/AZ31 composite under dry sliding wear condition. *Surf. Interfaces* **2017**, *6*, 143–153. [[CrossRef](#)]
23. Rengasamy, N.V.; Rajkumar, M.; Senthil Kumaran, S. Mining environment applications on Al 4032 - Zrb₂ and Tib₂ in-situ composites. *J. Alloy. Compd.* **2016**, *658*, 757–773. [[CrossRef](#)]
24. Rengasamy, N.V.; Rajkumar, M.; Senthil Kumaran, S. An analysis of mechanical properties and optimization of EDM process parameters of Al 4032 alloy reinforced with Zrb₂ and Tib₂ in-situ composites. *J. Alloy. Compd.* **2016**, *662*, 325–338. [[CrossRef](#)]
25. Paranthaman, P.; Gopal, P.M.; Kumar, N.S. Characterization of Economical Aluminium MMC Reinforced with Weld Slag Particles. In *Advances in Manufacturing Technology*; Springer: Singapore, 2019; pp. 9–16.
26. Kavimani, V.; Prakash, K.S.; Starvin, M.S.; Kalidas, B.; Viswamithran, V.; Arun, S.R. Tribo-Surface Characteristics and Wear Behaviour of SiCp@ r-GO/Mg Composite Worn under Varying Control Factor. *Silicon* **2019**, 1–11. [[CrossRef](#)]
27. Kumar, N.M.; Kumaran, S.S.; Kumaraswamidhas, L.A. High temperature investigation on EDM process of Al 2618 alloy reinforced with Si₃N₄, ALN and ZrB₂ in-situ composites. *J. Alloy. Compd.* **2016**, *663*, 755–768. [[CrossRef](#)]
28. Kumar, N.M.; Kumaran, S.S.; Kumaraswamidhas, L.A. An investigation of mechanical properties and material removal rate, tool wear rate in EDM machining process of AL2618 alloy reinforced with Si₃N₄, ALN and ZrB₂ in-situ composites. *J. Alloy. Compd.* **2015**, *650*, 318–327. [[CrossRef](#)]
29. Kumar, N.M.; Kumaran, S.S.; Kumaraswamidhas, L.A. Wear behaviour of Al 261 8 alloy reinforced with Si₃N₄, AlN and ZrB₂ in situ composites at elevated temperatures. *Alex. Eng. J.* **2016**, *55*, 19–36.

30. Kumar, N.M.; Kumaran, S.S.; Kumaraswamidhas, L.A. Aerospace application on Al 2618 with reinforced Si_3N_4 , ALN and ZrB_2 in-situ composites in-situ composites. *J. Alloy. Compd.* **2016**, *672*, 238–250. [[CrossRef](#)]
31. Kumar, N.M.; Kumaran, S.S.; Kumaraswamidhas, L.A. An Optimization of Erosive Wear on AA 2618 Reinforced with Si_3N_4 , ALN and ZrB_2 In Situ Composites. *Appl. Mech. Mater.* **2016**, *852*, 452–458. [[CrossRef](#)]
32. Selvaraj, S.K.; Nagarajan, M.K.; Kumaraswamidhas, L.A. An investigation of abrasive and erosion behaviour of AA 2618 reinforced with Si_3N_4 , ALN and ZrB_2 in-situ composites by using optimization techniques. *Arch. Civ. Mech. Eng.* **2017**, *17*, 43–54. [[CrossRef](#)]
33. Dolata, A.J. Tribological Properties of AlSi12-Al 2O_3 Interpenetrating Composite Layers in Comparison with Unreinforced Matrix Alloy. *Materials* **2017**, *10*, 1045. [[CrossRef](#)] [[PubMed](#)]
34. Toboła, D. Impact of Mechanical Processes as a Pre-Sulphonitriding Treatment on Tribology Properties of Selected P/M Tool Steels. *Materials* **2019**, *12*, 3431. [[CrossRef](#)] [[PubMed](#)]
35. Lenart, A.; Pawlus, P.; Dzierwa, A. The Effect of Disc Surface Topography on the Dry Gross Fretting Wear of an Equal-Hardness Steel Pair. *Materials* **2019**, *12*, 3250. [[CrossRef](#)] [[PubMed](#)]
36. Li, Y.; Wang, X.; Yang, S.; Hou, L.; Wei, Y.; Zhang, Z.; Yang, X. Investigation on Wear Behavior of Cryogenically Treated Ti-6Al-4V Titanium Alloy under Dry and Wet Conditions. *Materials* **2019**, *12*, 2850. [[CrossRef](#)] [[PubMed](#)]



© 2019 by the authors. Licensee MDPI, Basel, Switzerland. This article is an open access article distributed under the terms and conditions of the Creative Commons Attribution (CC BY) license (<http://creativecommons.org/licenses/by/4.0/>).